Computer Modeling in Engineering & Sciences
DOI:10.32604/cmes.2020.08989
Article

A New Method of Roughness Construction and Analysis of Construct Parameters

Hui Lu, Xinyue Duan, Minghai Xu*, Liang Gong and Bin Ding

College of New Energy, China University of Petroleum (East China), Qingdao, 266580, China
*Corresponding Author: Minghai Xu. Email: minghai@upc.edu.cn
Received: 31 October 2019; Accepted: 03 January 2020

Abstract: In micro-manufacturing, roughness is unavoidable due to the tolerance of micro-machining methods. Roughness in microchannel could have a significant influence on flow and heat transfer since the size of microchannel is very small. In our work, roughness is modeled as a superposition of waves. A simple Fourier series method is proposed to construct the rough surface. With this method, roughness is constructed on the bottom of the rectangular microchannel which has a hydraulic diameter of 0.5 mm. Two important parameters during roughness construction, triangulate size and correlation length are studied under the same relative roughness 1%. Results show that flow and heat transfer characteristics are not sensitive to triangulate size. While triangulate size is changing from 0.1 mm to 0.05 mm, the variations of pressure drop and average Nusselt number are less than 1%. Correlation length could influence the topography of roughness surface a lot, smaller correlation length will lead to more pressure drop and lower Nusselt number.

Keywords: Numerical simulation; nano/micro; electronic cooling; surface roughness

1 Introduction

Because of the power density growth of electronics, traditional cooling methods such as natural or forced air convection couldn't afford the cooling demands of high power electronics. As a much more efficient cooling method, liquid cooling method which uses microchannel heat sink to remove the massive heat on electronics becomes a trend [1–3]. During the machining and finishing process of microchannel, surface roughness is unavoidable. Different micro-machining methods such as electrical discharge machining (EDM), electrochemical machining (ECM), etching, micro-milling, etc., have machining tolerance varying from 10^{-2} μm to 5 μm [4–8]. Such absolute roughness could be neglected in the macro channel, but in the microchannel, due to the small feature dimension, roughness could have significant influence on flow and heat transfer compared to the macro channel. So it's necessary to study the influence of roughness on flow and heat transfer characteristics in the microchannel heat sink.

Experimental studies of roughness in microchannel have already been carried out by many researchers. Most experiments were focused on the comparison between smooth channel and rough channel. Qu et al. [9] experimentally studied water flow in trapezoidal silicon microchannel with hydraulic diameter ranging from

51 μm to 169 μm. Data show that friction in the rough microchannel is higher than conventional theory. Li et al. [10] studied rough steel microtubes with 3%–4% relative roughness and compared with smooth glass microtubes and silicon microtubes. They found that Poiseuille number in rough microtubes is increased by 15%–37%. Kandlikar et al. [11] used acid etching to change the roughness of microtubes of two different diameter 0.62 mm and 1.067 mm. For the 1.067 mm diameter tube, the effects of relative roughness varies from 0.178% to 0.225% are insignificant. For the 0.62 mm diameter tube, 0.3% relative roughness could apparently enhance the heat transfer and increase the pressure drop. Wu et al. [12] investigated 13 different trapezoidal silicon microchannels with relative roughness ranging from 0.003% to 1.09%, Nusselt number and apparent friction constant both increase with surface roughness under laminar flow. Dai et al. [13] reviewed 33 papers and 5569 experimental data points, flow and transition characteristics were summarized. 1% relative roughness is recommended as a threshold to divide smooth and rough for flow in microchannels, while 5% for macro tubes. Shapes of cross-section have little effect on friction and transition characteristics. From the previous studies, it could be concluded that the effects of roughness are significant in the microchannel, flow resistance and heat transfer efficiency are all related to roughness. But experiments could only obtain an average value of pressure drop or heat transfer intensity with uncertain errors.

Besides the experimental method, another commonly used method is numeric method. There are two main paths to model a rough surface, regular rough element method and random roughness method. Regular rough element method creates a rough surface by place cuboid, pyramid or other regular obstructions on a smooth surface. This method is easy to deploy, so many researchers chose this method to model roughness. Hu et al. [14] used cuboid elements to construct roughness, they found that geometry parameters such as height, spacing, size, and channel height have a strong effect on velocity distribution and pressure drop. Croce et al. [15] modeled roughness as a set of conical peaks on smooth surfaces. Influence of peak height, distance and Reynolds number are studied. They concluded that roughness has much more influence on pressure drop than heat transfer. Gamrat et al. [16] modeled roughness as cuboid elements and concluded that roughness increases the friction factor more than the heat transfer coefficient. Zhang et al. [17] used triangular, rectangular and semicircular roughness elements to construct rough surfaces. Effects of Reynolds number, roughness height, roughness spacing were investigated. Results show that triangular and semicircular elements have more influence on flow and heat transfer than rectangular elements. Both pressure drop and heat convection are increased.

Regular element method is an easy way to model a rough surface, but the flow and heat transfer are highly depending on the geometry shapes and parameters of roughness elements, too many parameters need to be considered. Therefore, some researchers were trying to find a more proper method to model random roughness. Random roughness method considers the physical characteristics of roughness and is much closer to real roughness than regular roughness. Chen et al. [18] modeled 2.5D roughness with Weierstrass-Mandelbrot function and studied under different Reynolds numbers, relative roughness and fractal dimension. Compared to the smooth channel, Poiseuille number is increasing linearly with Reynolds number. Another important conclusion is that under the same relative roughness, a larger fractal dimension which could yield more frequent variations results in larger pressure loss. Xiong [19] generated random roughness in microtube with Gaussian number generator. They found that Poiseuille number could still be predicted by conventional theory with the mean hydraulic diameter of rough microtube and roughness has a negligible effect on average Nusselt number. Guo et al. [20] modeled rough surface with regular rough elements, fractal function and random Gauss distribution in 2D and 3D. Their study shows that 2D roughness couldn't reveal the effects of real roughness. Simulation results in 3D indicate that both pressure drop and Nusselt number are increasing with roughness. Pelevicé et al. [21] generated rough surfaces with Gauss method and studied with lattice Boltzmann method, they also concluded that 2D roughness couldn't represent the 3D roughness. When relative roughness is 2.93%, Poiseuille number increases by up to 7%, heat transfer increases by up to 4%. Compared to model roughness as regular elements, model roughness with random feature is closer to reality and could obtain more reasonable results about the effects of roughness.

Concluded from the previous experiments and simulations, experiments could only obtain some flow and heat transfer features on the whole, simulations are still needed to understand the effects of roughness. In simulations, the most important part is to model the roughness. In this paper, a simple Fourier series method is proposed to model the roughness. This method is easy to deploy than Fourier transform method and considers the most significant feature of roughness: random and correlation. With this method, much more convincing results could be obtained compared to the traditional method that model roughness as regular rough elements or completely random method that ignore the correlation feature of roughness. Two key parameters in roughness construction, triangulate size and correlation length are studied under the same relative roughness 1% to evaluate the usability of this roughness model.

2 Roughness Model

Since any surface include rough surface could be seen as superposition of simple surfaces with different frequencies and phases, the 2D Fourier series is used to model the rough surface mathematically. Eq. (1) is the complex form of the 2D Fourier series.

$$Z(x,y) = \sum_{m=-\infty}^{+\infty} \sum_{n=-\infty}^{+\infty} c_{mn} e^{-in\omega_x x} e^{-im\omega_y y} \tag{1}$$

$$c_{mn} = \frac{a_{mn} + ib_{mn}}{2} \tag{2}$$

$Z(x, y)$ here is the expression function of rough surface. ω_x and ω_y are cut off frequencies to ensure the period length is far larger than the geometry dimension. To solve c_{mn}, amplitude spectrum $A(n\omega_x, n\omega_y)$ and phase spectrum $\varphi\,(n\omega_x, n\omega_y)$ are introduced, $\varphi\,(n\omega_x, n\omega_y)$ is random from 0 to 2π (isotropic roughness), $A(n\omega_x, n\omega_y)$ is the square root of power spectrum:

$$R(r) = \sigma^2 e^{-\frac{r^2}{l^2}} \tag{3}$$

$$A\left(n\omega_x, n\omega_y\right) = \sqrt{F(R(r))} = \sqrt{F\left(\sigma^2 e^{-\frac{r^2}{l^2}}\right)} = \sqrt{l_x l_y \sigma^2 \pi e^{-\frac{n^2\omega_x^2 l_x^2}{4}} e^{-\frac{m^2\omega_y^2 l_y^2}{4}}} \tag{4}$$

$R(r)$ is the exponential correlation function, r is the distance between two points on a rough surface, l_x and l_y are correlation length. σ is standard deviation. Since $Z(x, y)$ is always a real number in our case, the real form of 2D Fourier series is used to generate roughness:

$$\begin{aligned} Z(x,y) = \sum_{m=0}^{\infty}\sum_{n=0}^{\infty} & \left(a_{n,m} + a_{n,-m}\right)\cos n\omega_x x \cos m\omega_y y - \left(b_{n,m} + b_{n,-m}\right)\sin n\omega_x x \cos m\omega_y y \\ & + \left(a_{n,m} + a_{n,-m}\right)\cos n\omega_x x \sin m\omega_y y + \left(b_{n,m} + b_{n,-m}\right)\sin n\omega_x x \sin m\omega_y y \end{aligned} \tag{5}$$

a and b in Eq. 5 could be obtained from A and φ. $a = 2A\cos\varphi$, $b = 2A\sin\varphi$.

With above method, steps to generate roughness on a surface is listing below:

1. Triangulate the smooth surface to triangular mesh.
2. With give parameters, calculate $Z(x,y)$ to obtain the offset Z at nodes of smooth surface.
3. Move the nodes of triangular mesh to produce roughness.

3 Microchannel Description

Flat microchannel heat sink with 1 mm × 1 mm × 2 mm dimensions is used in this study. Water is chosen as working fluid and cooper is the material of microchannel heat sink. As shown in Fig. 1, the microchannel is in the center of the heat sink and has a hydraulic diameter of 0.5 mm. Constant heat flux is employed on the bottom of the microchannel heat sink. Roughness is generated on the bottom surface of the microchannel (marked as gray). Different triangulate sizes from 0.01 mm to 0.05 mm, different correlation lengths from 0.01 mm to 0.07 mm are used as parameters to generate roughness on this geometry model. Both fluid and solid domains are included in the simulation.

4 Numeric Method

4.1 Governing Equations

To simplify the problem, fluid flow is assumed as steady, incompressible laminar flow with constant properties. Gravity and viscous heating are not considered. Continuity momentum and energy equations are written as:

Continuity:

$$\frac{\partial u}{\partial x} + \frac{\partial v}{\partial y} + \frac{\partial w}{\partial z} = 0 \tag{6}$$

Momentum:

$$\frac{\partial (uu)}{\partial x} + \frac{\partial (vu)}{\partial y} + \frac{\partial (wu)}{\partial z} = v\left(\frac{\partial^2 u}{\partial x^2} + \frac{\partial^2 u}{\partial y^2} + \frac{\partial^2 u}{\partial z^2}\right) - \frac{1}{\rho}\frac{\partial p}{\partial x} \tag{7}$$

$$\frac{\partial (uv)}{\partial x} + \frac{\partial (vv)}{\partial y} + \frac{\partial (wv)}{\partial z} = v\left(\frac{\partial^2 v}{\partial x^2} + \frac{\partial^2 v}{\partial y^2} + \frac{\partial^2 v}{\partial z^2}\right) - \frac{1}{\rho}\frac{\partial p}{\partial y} \tag{8}$$

$$\frac{\partial (uw)}{\partial x} + \frac{\partial (vw)}{\partial y} + \frac{\partial (ww)}{\partial z} = v\left(\frac{\partial^2 w}{\partial x^2} + \frac{\partial^2 w}{\partial y^2} + \frac{\partial^2 w}{\partial z^2}\right) - \frac{1}{\rho}\frac{\partial p}{\partial z} \tag{9}$$

Energy:

$$\frac{\partial (uT)}{\partial x} + \frac{\partial (vT)}{\partial y} + \frac{\partial (wT)}{\partial z} = \frac{\lambda}{\rho c_p}\left(\frac{\partial^2 T}{\partial x^2} + \frac{\partial^2 T}{\partial y^2} + \frac{\partial^2 T}{\partial z^2}\right) \tag{10}$$

where x, y and z are coordinates. u, v and w are velocity magnitude on x, y and z direction. ρ is the density of fluid or solid. p is pressure. c_p is fluid specific heat and λ is thermal conductivity of the fluid or solid.

4.2 Boundary Condition

For all cases, periodic flow conditions are employed on the inlet and outlet (marked as blue ones in Fig. 1) . Heating source on the bottom of heat sink is 0.2 W/mm^2 (marked as pink in Fig. 1). Other walls are adiabatic and there is no velocity slip on the wall. Average inlet temperature is 300 K, Reynolds number is 500.

4.3 Auxiliary Relations

The average Nusselt number Nu is defined as

$$Nu = \frac{hD_e}{\lambda_f} = \frac{QD_e}{S_{\text{wall}}\lambda_f\left(T_{\text{wall}} - T_f\right)} \tag{11}$$

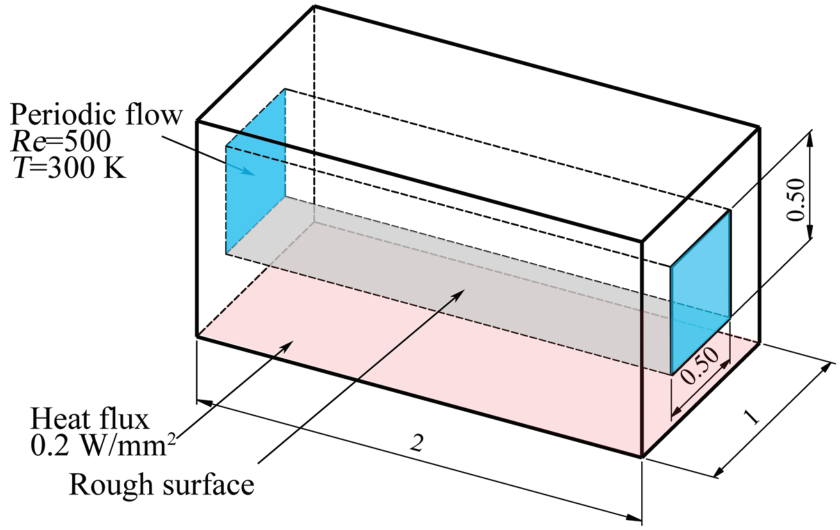

Figure 1: Schematic of the geometry model (mm)

where h is the heat transfer coefficient, Q is the total heating power. S_{wall} is the area of fluid-solid interface. T_{wall} is the average temperature of fluid-solid interface and T_f is the average fluid temperature. The average wall temperature T_{wall} is defined as

$$T_{\text{wall}} = \frac{\iint\limits_{\text{wall}} TdS}{S_{\text{wall}}} = \frac{\iint\limits_{\text{wall}} TdS}{\iint\limits_{\text{wall}} dS} \tag{12}$$

The average fluid temperature T_{fluid} is evaluated as

$$T_f = \frac{\iiint\limits_{\text{fluid}} TdV}{\iiint\limits_{\text{fluid}} dV} \tag{13}$$

4.4 Mesh Independency Check

Hexahedral mesh with refinement near the rough surface of the microchannel is used as computational grid as shown in Fig. 2. Mesh independency is checked carefully on the case with 0.01 mm correlation length which has the smallest roughness feature size.

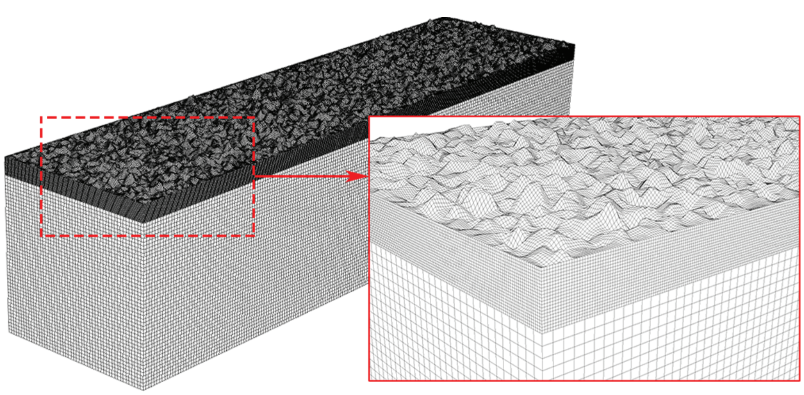

Figure 2: Mesh of the fluid zone with local refinement near rough surface

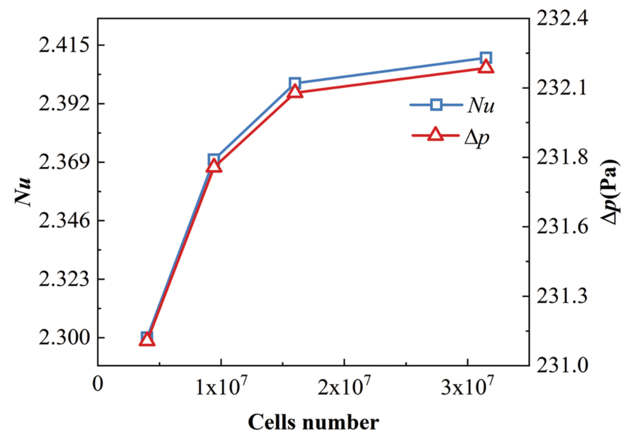

Figure 3: Mesh independency check of the case with 0.01 mm correlation length

Fig. 3 shows the variation of pressure drop and Nusselt number while cell number grows. The changes of pressure drop and Nusselt number are less than 1% while cell number changes from 16.2 million to 31.5 million. As a result, mesh size configuration of 16.2 million is used for all cases to obtain a mesh independent result.

5 Results

5.1 Influence of Geometry Triangulate Size

The first step to generate roughness on a surface is to triangulate that surface. After the surface is triangulated, that surface is converted to mesh which consists of triangles and nodes. It's much easier to generate roughness on triangular meshes by offsetting the nodes. The triangulate size means the edge length of triangles or the distance between two adjacent nodes. Smaller triangulate size could capture the feature of roughness more precisely and the roughness surface is closer to a continuous surface, but more fine mesh is needed. Also, the triangulate size could influence the contact characteristics of a rough surface, when triangulate size is large, that means the contact of the rough surface is sharp.

As shown in Fig. 4, roughness is generated on the bottom faces of the microchannel with five different triangulate sizes and identical correlation length 0.05 mm. The surface profile is the same in these five cases and average relative roughness is 1%, also the same. The only difference between these surfaces is triangulate size. It is seen that with smaller correlation size, the surface is smoother and contains more details that defines a rough surface. When the correlation length is growing, there is possibility to lose the key features of roughness surface, peaks and valleys on the surface are not that clear. The Probability density distribution of absolute roughness with different triangulate sizes are shown in Fig. 5. Roughness should obey Gauss distribution perfectly but because of the simplify of the geometry which uses triangles to represent

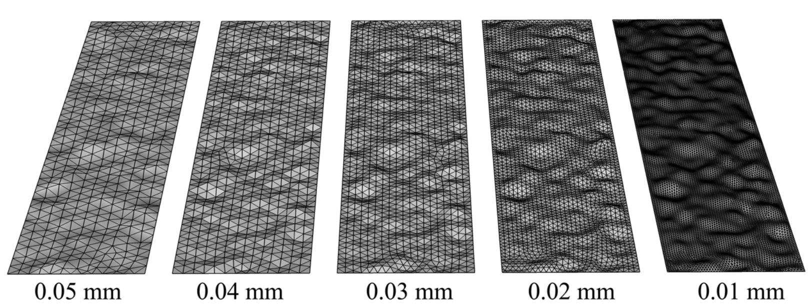

Figure 4: Rough surfaces of microchannel with 1% roughness and different triangulate sizes

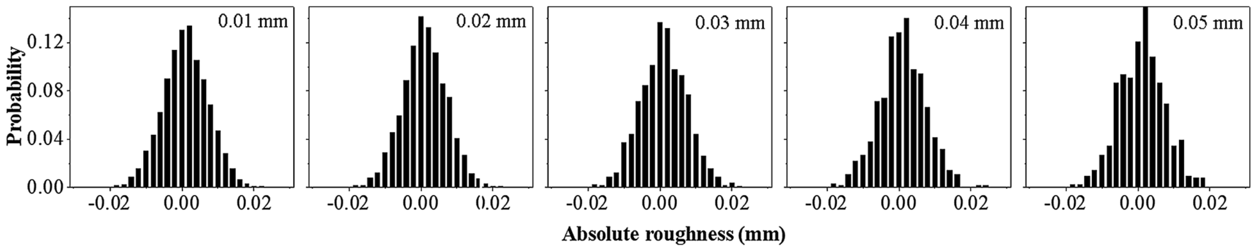

Figure 5: Probability density distribution of absolute roughness with different triangulate sizes

continuous surfaces, the distributions are not exactly Gauss distribution. The smaller of the triangulate size, the closer to exact Gauss distribution. The cosine similarity of probability distribution between the cases with 0.01 mm and 0.05 mm is 0.989, which means they are highly similar to each other on the distribution of roughness. To find out the actual influence of triangulate size on local and average flow and heat transfer characteristics, these five cases are numerically studied using the same boundary conditions.

The influence of triangulate size on pressure drop and Average Nusselt number is shown in Fig. 6. Compared to the smooth channel, pressure drop in rough channel has a minimal increase of about 1%, while the Nusselt number almost unchanged. Both pressure drop and average Nusselt number are not sensitive to triangulate size. When the triangulate size is decreasing, the wetting length of the channel cross-section is growing and causes minimal raise in flow resistance. The changes in pressure drop and Nusselt number are 0.35% and 0.15% respectively while triangulate size varies from 0.01 mm to 0.05 mm. So the influence of triangle size on pressure drop and average Nusselt number could be neglected on this view. Local Nusselt number distribution and streamline near the rough surface is plotted in Fig. 7, comparing these five cases, it is seen that the case with smaller triangulate size has better precision on local Nusselt number, especially on local peaks of rough structures. On the whole, the local Nusselt distribution is much the same. Since there's no visible difference in streamline between these five cases, the streamline plotted in Fig. 7 is only for 0.01 mm triangulate size. The streamline is disturbed by the roughness structure and the fluid impinges on the roughness structure, on the peaks of the rough structures, there is higher local Nusselt number and flow resistance, while in the valleys of roughness structures, there is lower local Nusselt number due to the low fluid velocity.

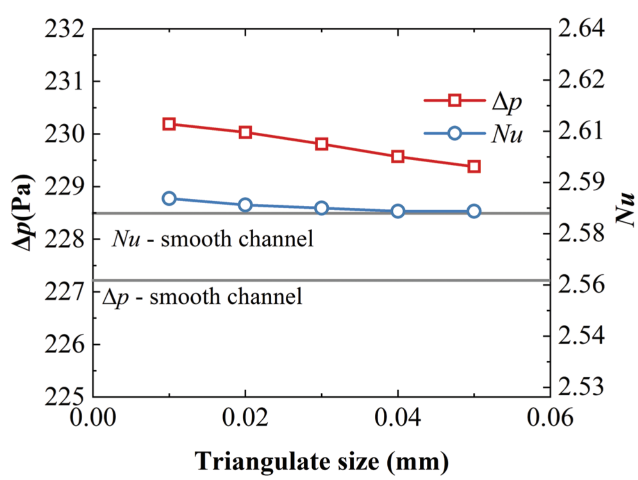

Figure 6: Influence of triangulate size on pressure drop and Nusselt number

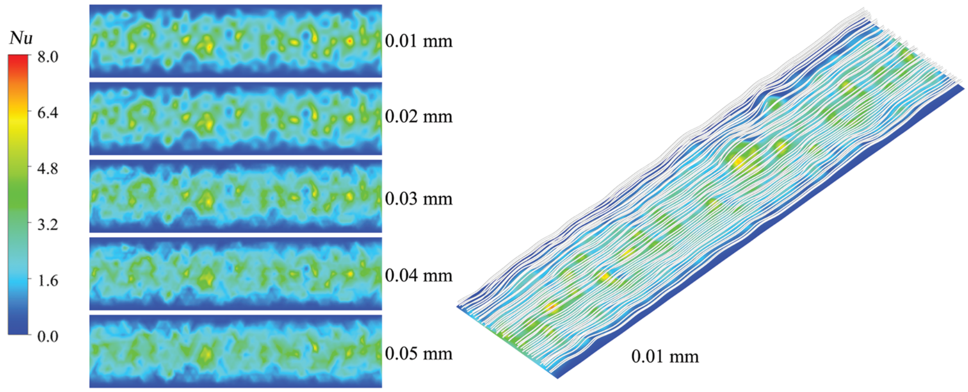

Figure 7: Local Nusselt number on the rough surfaces and streamlines near the rough surfaces (different triangulate sizes)

From the above analysis, average Nusselt number and pressure drop are not sensitive to triangulate size while triangulate size is smaller than correlation length. Minimal influence of triangulate size on local Nusselt number is observed. For computational resource saving, triangulate size could set equal to correlation length if local values are not excessively concerned.

5.2 Influence of Correlation Length

Correlation length is a very important parameter in the roughness generation process. In the actual machining process, correlation length is related to material property, micro machining method, polishing method, and other manufacture conditions. It's difficult to predict correlation length and the best path to obtain correlation length is experimental measurement. This part discusses the influence of correlation length only in assumption and ignores the actual degree of correlation length. Seven different cases, with correlation length varies from 0.01 mm to 0.07 mm, are numerically studied. All of the cases have equivalent relative roughness 1% and triangulate size 0.01 mm. The bottom faces of microchannel with different correlation lengths are shown in Fig. 8.

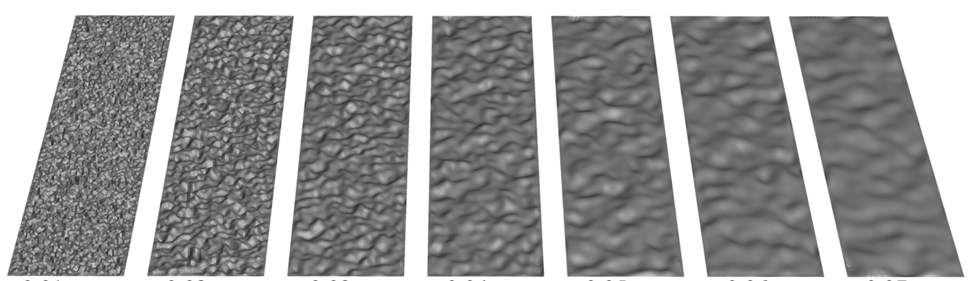

Figure 8: Rough surfaces of microchannel with different correlation length and the same relative roughness 1%

Physically, correlation length represents the influence range of one roughness point on other points, in other word, correlation length is a measurement of the constraint between the roughness of neighboring points. As shown in Fig. 8, with the growth of correlation length, the constraint between points on rough surface is stronger and there are fewer sudden peaks and valleys. With the decrease of correlation length, constraint between points are weaker and there will be much more random fluctuations on the rough surfaces. There is huge topography changes when the correlation length is varying. Influence of correlation length on geometry, flow and heat transfer characteristics are listed in Tab. 1. With the decrease of correlation length, there are more peaks and valleys in smaller scale and that makes the surface area of roughness fast-growing. Also, the scale down of the roughness structure leads to the growth of the wetted perimeter and cross-section area. Hydraulic diameter is decreasing during this process and causes drag increase. It is seen in Fig. 9 that pressure drop has an approximately linear relation with correlation length within our computed range. Correlation length also affects the heat transfer characteristics. There are two adverse effects of roughness, on one hand, roughness expands the surface area of heat convection, on the other hand, the valleys that capture fluid in them could decrease the heat convection and bring additional thermal resistance. The overall effect of those two adverse factors could be either enhance or weaken the heat convection. It is shown in Tab. 1 that average Nusselt number is decreasing with correlation length and could be either larger or smaller than the smooth channel. While correlation length is bigger than 0.02 mm, heat transfer is slightly enhanced. While correlation length is smaller than 0.02 mm, the enhancement is disappearing. The maximum enhancement of average Nusselt number occurs at the maximum correlation length and the increase is 1.1%. Average Nusselt number has a linear relation with surface area A. Besides the influence of roughness on average Nusselt number, the actual influence of roughness on the most important parameter in electronics cooling - maximum temperature T_{max} is quite small.

Table 1: Compare of models with different correlation length

Correlation length (mm)	A (mm^2)	Δp (Pa)	Nu	T_{max} (K)
0.01	4.311	232.20	2.41	323.60
0.02	4.150	231.66	2.50	323.58
0.03	4.076	231.10	2.58	323.27
0.04	4.050	230.64	2.58	323.38
0.05	4.034	230.22	2.60	323.27
0.06	4.027	229.99	2.60	323.26
0.07	4.019	229.69	2.61	232.26
Smooth	4.000	227.23	2.58	323.40

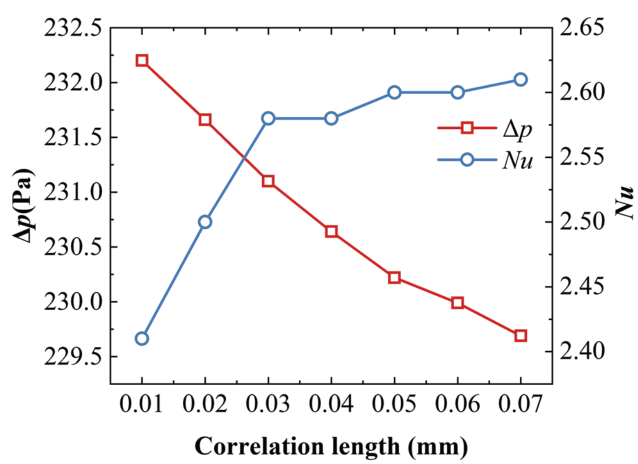

Figure 9: Influence of correlation length on pressure drop and Nusselt number

Local Nusselt number distribution on the bottom rough surfaces is plotted in Fig. 10. It is seen that correlation length affects the local heat transfer a lot. Despite the scale of correlation length, heat transfer on the peaks of the roughness structure is enhanced because the fluid impinges on the peaks. While the correlation length is decreasing, the size of cavities on the rough surface becomes smaller. It's more difficult for fluid to flow into the cavities and that weakens the heat convection. According to our calculation, while the correlation length is 0.07 mm, average velocity gradient on the rough surface is 1.47 times larger than that correlation length is 0.01 mm.

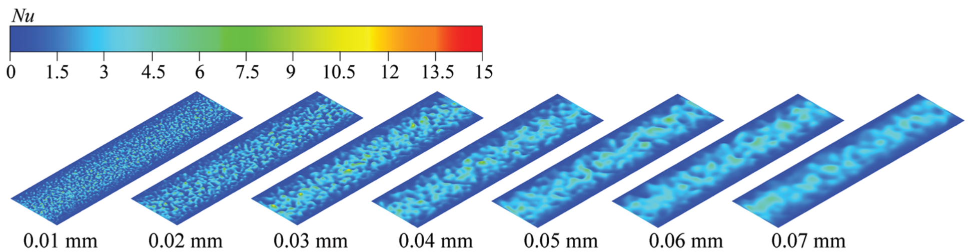

Figure 10: Local Nusselt number on the rough surfaces of microchannel and streamlines near the rough surfaces

While correlation length varies from 0.01 mm to 0.07 mm, the pressure drop and average Nusselt number changed by 2.2% and 7.7% respectively. The heat convection is more sensitive to correlation length than flow resistance. Though the average Nusselt number has some reduction while correlation length is decreasing, the growth of the heat convection area balanced this reduction in average Nusselt number. The final cooling effect of microchannel almost the same since the maximum temperature of the heat sink barely changes.

6 Conclusions

A simple Fourier series method which considered the random and correlation features of roughness is used to construct roughness on the bottom face of flat microchannel heat sink with 0.5 mm hydraulic diameter. The smooth model is triangulated first and then processed in our software to generate roughness. Effect of triangulate size and correlation length are studied under the same relative roughness 1% and the same Reynolds number 500. The main conclusions are listed below:

1. Triangulate size, which is the precision of roughness structure and could also represent the contact feature of rough surface, has little influence (within 1%) on the overall flow and heat transfer characteristics of microchannel.
2. Correlation length, which is a parameter determined by machining and finishing process, has a limited influence on flow and heat transfer. While correlation length varies from 0.01 mm to 0.07 mm, flow resistance decreased by 2.2%, average Nusselt number increased by 7.7%.
3. Roughness could be either beneficial or helpless to the thermal performance of microchannel under different correlation length.

Since there is almost no transverse flow in a rectangular channel, the velocity gradient on the rough surface is quite small, so the effects of roughness are not that obvious. The future work should be focused on complex channel like wavy or dimpled channel that has more secondary flow.

Funding Statement: This work is financially supported by the Natural Science Foundation of China (No. 51676208) and the Fundamental Research Funds for the Central Universities (No.18CX07012A and

No. 19CX05002A). The authors are also grateful for the support from the Major Program of the Natural Science Foundation of Shandong Province (No. ZR2019ZD11).

Conflicts of Interest: The authors declare that they have no conflicts of interest to report regarding the present study.

References

1. Gong, L., Xu, Y. P., Ding, B., Zhang, Z. H., Huang, Z. Q. (2020). Thermal management and structural parameters optimization of MCM-BGA 3D package model. *International Journal of Thermal Sciences, 147,* 106120. DOI 10.1016/j.ijthermalsci.2019.106120.
2. Gong, L., Li, Y., Bai, Z., Xu, M. H. (2018). Thermal performance of micro-channel heat sink with metallic porous/solid compound fin design. *Applied Thermal Engineering, 137,* 288–295. DOI 10.1016/j.applthermaleng.2018.03.065.
3. Xu, M. H., Lu, H., Gong, L., Chai, J. C., Duan, X. Y. (2016). Parametric numerical study of the flow and heat transfer in microchannel with dimples. *International Communications in Heat and Mass Transfer, 76,* 348–357. DOI 10.1016/j.icheatmasstransfer.2016.06.002.
4. Richard, J., Demellayer, R. (2013). Micro-EDM-milling development of new machining technology for micro-machining. *Procedia CIRP, 6,* 292–296. DOI 10.1016/j.procir.2013.03.023.
5. Chavoshi, S. Z., Luo, X. C. (2014). Hybrid micro-machining processes: a review. *Precision Engineering, 41,* 1–23. DOI 10.1016/j.precisioneng.2015.03.001.
6. Lai, L. J., Zhou, H., Zhu, L. M. (2016). Fabrication of microlens array on silicon surface using electrochemical wet stamping technique. *Applied Surface Science, 364,* 442–445. DOI 10.1016/j.apsusc.2015.12.085.
7. Zhang, S. J., To, S., Wang, S. J., Zhu, Z. W. (2015). A review of surface roughness generation in ultra-precision machining. *International Journal of Machine Tools and Manufacture, 91,* 76–95. DOI 10.1016/j.ijmachtools.2015.02.001.
8. Yang, C. R., Chen, P. Y., Chiou, Y. C., Lee, R. T. (2005). Effects of mechanical agitation and surfactant additive on silicon anisotropic etching in alkaline KOH solution. *Sensors and Actuators A: Physical, 119(1),* 263–270. DOI 10.1016/j.sna.2004.07.015.
9. Qu, W. L., Mala, M., Mala, G. M., Li, D. Q. (2000). Pressure-driven water flows in trapezoidal silicon microchannels. *International Journal of Heat and Mass Transfer, 43(3),* 353–364. DOI 10.1016/S0017-9310(00)00045-4.
10. Li, Z. X., Du, D. X., Guo, Z. Y. (2003). Experimental study of flow characteristics of liquid in circular microtubes. *Microscale Thermophysical Engineering, 7(3),* 253–265. DOI 10.1080/10893950390219083.
11. Kandlikar, S. G., Joshi, S., Tian, S. R. (2003). Effect of surface roughness on heat transfer and fluid flow characteristics at low Reynolds numbers in small diameter tubes. *Heat Transfer Engineering, 24(3),* 4–16. DOI 10.1080/01457630304069.
12. Wu, H. Y., Cheng, P. (2003). An experimental study of convective heat transfer in silicon microchannels with different surface conditions. *International Journal of Heat and Mass Transfer, 46(14),* 2547–2556. DOI 10.1016/S0017-9310(03)00035-8.
13. Dai, B. M., Li, M. X., Ma, Y. T. (2014). Effect of surface roughness on liquid friction and transition characteristics in micro- and mini-channels. *Applied Thermal Engineering, 67(1–2),* 283–293. DOI 10.1016/j.applthermaleng.2014.03.028.
14. Hu, Y. D., Werner, C., Li, D. Q. (2003). Influence of three-dimensional roughness on pressure-driven flow through microchannels. *Journal of Fluids Engineering, 125(5),* 871–879. DOI 10.1115/1.1598993.
15. Croce, G., D'agaro, P., Nonino, C. (2007). Three-dimensional roughness effect on microchannel heat transfer and pressure drop. *International Journal of Heat and Mass Transfer, 50(25–26),* 5249–5259. DOI 10.1016/j.ijheatmasstransfer.2007.06.021.
16. Gamrat, G., Favre-Marinet, M., Le Person, S. (2009). Modelling of roughness effects on heat transfer in thermally fully-developed laminar flows through microchannels. *International Journal of Thermal Sciences, 48(12),* 2203–2214. DOI 10.1016/j.ijthermalsci.2009.04.006.

17. Zhang, C. B., Chen, Y. P., Shi, M. H. (2010). Effects of roughness elements on laminar flow and heat transfer in microchannels. *Chemical Engineering and Processing: Process Intensification, 49(11),* 1188–1192. DOI 10.1016/j.cep.2010.08.022.
18. Chen, Y. P., Zhang, C. B., Shi, M. H., Peterson, G. P. (2009). Role of surface roughness characterized by fractal geometry on laminar flow in microchannels. *Physical Review E, 80(2),* 026301. DOI 10.1103/PhysRevE.80.026301.
19. Xiong, R. Q., Chung, J. N. (2010). A new model for three-dimensional random roughness effect on friction factor and heat transfer in micro tubes. *International Journal of Heat and Mass Transfer, 53(15–16),* 3284–3291. DOI 10.1016/j.ijheatmasstransfer.2010.02.050.
20. Guo, L., Xu, H. J., Gong, L. (2015). Influence of wall roughness models on fluid flow and heat transfer in microchannels. *Applied Thermal Engineering, 84,* 399–408. DOI 10.1016/j.applthermaleng.2015.04.001.
21. Pelević, N., van der Meer, T. H. (2016). Heat transfer and pressure drop in microchannels with random roughness. *International Journal of Thermal Sciences, 99,* 125–135. DOI 10.1016/j.ijthermalsci.2015.08.012.